Abstract: The cheetah is capable of a top speed of 29 ms)1 compared to the maximum speed of 17 ms)1 achieved by theracing greyhound. In this study of the hindlimb and in the accompanying paper on the forelimb we have quanti-fied the musculoskeletal anatomy of the cheetah and greyhound and compared them to identify any differencesthat may account for this variation in their locomotor abilities. Specifically, bone length, mass and mid-shaftdiameter were measured, along with muscle mass, fascicle lengths, pennation angles and moment arms to enableestimates of maximal isometric force, joint torques and joint rotational velocities to be calculated. Surprisingly thecheetahs had a smaller volume of hip extensor musculature than the greyhounds, and we therefore propose thatthe cheetah powers acceleration using its extensive back musculature. The cheetahs also had an extremely powerfulpsoas muscle which could help to resist the pitching moments around the hip associated with fast accelerations.The hindlimb bones were proportionally longer and heavier, enabling the cheetah to take longer stridesand potentially resist higher peak limb forces. The cheetah therefore possesses several unique adaptations forhigh-speed locomotion and fast accelerations, when compared to the racing greyhound.Key words acinonyx; anatomy; cheetah; hindlimb; muscle; speed.

# Functional anatomy of the cheetah (*Acinonyx jubatus*) hindlimb

Penny E. Hudson,[1] Sandra A. Corr,[1]* Rachel C. Payne-Davis,[1] Sinead N. Clancy,[1]* Emily Lane[2] and Alan M. Wilson[1]

[1]*Structure and Motion Laboratory, The Royal Veterinary College, University of London, Hawkshead Lane, North Mymms, Hatfield, Hertfordshire, UK*
[2]*Research Department of the National Zoological Gardens of South Africa, Pretoria, South Africa*

## Abstract

The cheetah is capable of a top speed of 29 ms$^{-1}$ compared to the maximum speed of 17 ms$^{-1}$ achieved by the racing greyhound. In this study of the hindlimb and in the accompanying paper on the forelimb we have quantified the musculoskeletal anatomy of the cheetah and greyhound and compared them to identify any differences that may account for this variation in their locomotor abilities. Specifically, bone length, mass and mid-shaft diameter were measured, along with muscle mass, fascicle lengths, pennation angles and moment arms to enable estimates of maximal isometric force, joint torques and joint rotational velocities to be calculated. Surprisingly the cheetahs had a smaller volume of hip extensor musculature than the greyhounds, and we therefore propose that the cheetah powers acceleration using its extensive back musculature. The cheetahs also had an extremely powerful psoas muscle which could help to resist the pitching moments around the hip associated with fast accelerations. The hindlimb bones were proportionally longer and heavier, enabling the cheetah to take longer strides and potentially resist higher peak limb forces. The cheetah therefore possesses several unique adaptations for high-speed locomotion and fast accelerations, when compared to the racing greyhound.

**Key words** acinonyx; anatomy; cheetah; hindlimb; muscle; speed.

## Introduction

High-speed locomotion is essential for the survival and success of many species for both prey capture and escape from predatory attacks (Alexander, 2003). The cheetah (*Acinonyx jubatus*) is widely acknowledged as the fastest living land mammal, capable of speeds up to 29 ms$^{-1}$ (Sharp, 1997). The greyhound (*Canis familiaris*) has been selectively bred for high-speed locomotion yet can only attain speeds of 17 ms$^{-1}$ during a race (Usherwood & Wilson, 2005), despite both animals having a similar mass and gross morphology. Here we investigate the hindlimb musculoskeletal anatomy of both species to understand how the cheetah achieves such remarkable speeds.

Through the examination of the musculoskeletal anatomy of an animal it is possible to gain insight into its loco-motor capabilities. Measurements of muscle mass enable calculations of muscle volume, to which power is directly proportional (Zajac, 1989). The internal architecture of a muscle, i.e. fibre lengths and pennation angles, can also be measured to calculate the maximal isometric force ($F_{max}$) that a muscle can achieve. However, to truly understand how muscle anatomy corresponds to an animal's locomotor abilities, muscle moment arms must be considered.

The moment arm of a muscle is defined as the perpendicular distance from the joint centre of rotation to the line of action of the muscle, which can vary with changes in joint angle (Landsmeer, 1961; An et al. 1981; Spoor & van Leeuwen, 1992). Through measuring the muscle's moment arm we can convert the linear forces of a muscle to rotational joint moments, which act to resist external forces and move the limb. One of the major functions of locomotor muscle is to support the body weight of the animal by resisting the ground reaction force joint moments during stance. To support body weight, an impulse must be applied to the ground (during stance) that is equal in magnitude to the product of the animal's body weight and stride time (Alexander & Jayes, 1978). With increasing speed, an animal's duty factor (proportion of the stride that the feet are in contact with the ground) decreases, and therefore to maintain the impulse required to support body weight, the peak ground reaction force must increase

(Witte et al. 2006). It is therefore crucial for high-speed predators such as the cheetah to be able to generate large muscle joint torques to resist this force. Another requirement of high-speed locomotion is the ability to swing the limb rapidly and reposition it for the next stride. This is dependent on several factors: the limb's inertia (Lee et al. 2004), the internal architecture of the muscles (a long-fibred muscle has more sarcomeres in series enabling it to contract at a high velocity), and the muscle moment arms (a short moment arm enables greater changes in the joint rotation for a given change in muscle length).

The hindlimb anatomy of other high-speed animals has been studied in detail (Payne et al. 2005; Smith et al. 2006, 2007; Williams et al. 2008a; Williams et al. 2008b), and several common anatomical features have been noted. In all cases, a proximal to distal reduction in muscle mass was observed, with many of the distal muscles being in series with long tendons. This will reduce the inertia of the limb and therefore the amount of muscular work required to swing the limb. A trend for a large volume of powerful hip extensor musculature, which will aid acceleration, was also apparent (Usherwood & Wilson, 2005 Williams 2008b; Williams 2009b). This was particularly apparent in the study of Williams et al. (2008a,b), which compared the anatomy of mixed-breed dogs and greyhounds.

Here we aim to describe and quantify the musculoskeletal anatomy of the cheetah and compare this with published data on the racing greyhound to provide insight into how the fastest living land mammal achieves such high speeds.

## Materials and methods

### Cheetahs

Eight cheetah cadavers were collected and frozen (−20 °C) within 24 h of death by the Anne Van Dyk Cheetah Centre and the research department of the National Zoological Gardens of South Africa. All known subject information is provided in Table 1. Prior to dissection, the cadavers were stored at 4 °C for 48 h, or until defrosted. The right hindlimb of each cadaver was dissected to obtain measurements of muscle architecture, and moment arms of the major muscles were obtained for subjects 4–8 inclusive.

### Greyhounds

Three greyhound cadavers were obtained from greyhound racing track vets, and stored as previously described. Measurements of muscle architecture were obtained from them and pooled with published data on greyhound anatomy (Williams et al. 2008a,b) for discussion and comparison.

The ages of some subjects were unknown; however, all were fully mature, and the greyhounds had been racing and physically active until killed. All subjects died of causes unrelated to the study and were free of any gross musculoskeletal pathology that may have affected the results.

### Muscle architecture

All limbs were skinned and the surrounding fascia removed. Muscles were then systematically identified according to their origins and insertions and removed. The mass of each muscle

**Table 1** Known subject information.

| Subject | Age (years) | Gender | Body mass (kg) | Femur | | | Tibia | | |
|---|---|---|---|---|---|---|---|---|---|
| | | | | Length (mm) | Mass (g) | Diameter (mm) | Length (mm) | Mass (g) | Diameter (mm) |
| Cheetah 1 | 8.5 | Female | – | – | – | – | – | – | – |
| Cheetah 2 | 15.5 | Female | – | – | – | – | – | – | – |
| Cheetah 3 | 11.5 | Male | – | – | – | – | – | – | – |
| Cheetah 4 | 13.5 | Male | 31.0 | 294 | 258 | 23.0 | 298 | 196 | 21.5 |
| Cheetah 5 | 12 | Female | 29.5 | 267 | 189 | 21.6 | 278 | 156 | 20.3 |
| Cheetah 6 | 6 | Male | 27.5 | 281 | 210 | 21.6 | 287 | 160 | 21.9 |
| Cheetah 7 | 12.5 | Male | 32.0 | 282 | 264 | 23.0 | 284 | 188 | 20.4 |
| Cheetah 8 | 6.5 | Female | 45.5 | 262 | 196 | 22.7 | 262 | 152 | 18.4 |
| Greyhound 1 | – | Female | 25.0 | 236 | 153 | 16.6 | 250 | 118 | 17.5 |
| Greyhound 2 | – | Male | 28.0 | 235 | 147 | 16.4 | 249 | 113 | 17.6 |
| Greyhound 3 | – | Male | 29.0 | 228 | 146 | 16.2 | 242 | 110 | 17.2 |
| Greyhound 4 | – | Female | 27.0 | 190 | – | – | 230 | – | – |
| Greyhound 5 | – | Male | 33.0 | – | – | – | – | – | – |
| Greyhound 6 | – | Male | 34.0 | 200 | – | – | 270 | – | – |
| Greyhound 7 | – | Male | 33.0 | 205 | – | – | 270 | – | – |
| Greyhound 8 | – | Male | 28.0 | 200 | – | – | 260 | – | – |
| Greyhound 9 | – | Male | 33.0 | – | – | – | – | – | – |

Greyhounds 1–3 were dissected in this study, and greyhounds 4–9 were from data published by Williams (2008). The length, mass and mid-shaft diameter of the bones of each individual are also given.

**Table 2** Muscle moment arms (MAs): maximum, minimum and mid-stance MAs for the cheetah and maximum MAs for the greyhound (Williams, 2008).

| Joint | Muscle | Cheetah | | | | | | Greyhound |
|---|---|---|---|---|---|---|---|---|
| | | Max. MA | | Min. MA | | Mid-stance MA | | Max. MA |
| Hip | Biceps femoris | **16.7** | *2.5* | **2.4** | *0.6* | **7.1** | *1.2* | 2.9 |
| Hip | Rectus femoris | **4.7** | *0.2* | **4.7** | *0.2* | **4.7** | *0.2* | 2.4 |
| Hip | Semimembranosus | **19.4** | *3.3* | **5.0** | *0.9* | **9.7** | *1.6* | 6 |
| Hip | Semitendinosus | **18.1** | *1.5* | **5.4** | *1.3* | **9.6** | *0.5* | 10.8 |
| Hip | Tensor fascia latae | **12.5** | *1.9* | **5.5** | *1.2* | **7.8** | *1.3* | 13.6 |
| Stifle | Biceps femoris | **1.2** | *0.2* | **1.2** | *0.2* | **1.2** | *0.2* | 0.4 |
| Stifle | Gastrocnemius | **4.6** | *0.2* | **4.6** | *0.2* | **4.6** | *0.2* | 1.6 |
| Stifle | Rectus femoris | **3.3** | *0.6* | **3.3** | *0.6* | **3.3** | *0.6* | 2.4 |
| Stifle | Semimembranosus | **1.6** | *0.2* | **1.6** | *0.2* | **1.6** | *0.2* | 0.8 |
| Stifle | Semitendinosus | **10.9** | *0.9* | **3.6** | *0.7* | **8.5** | *0.3* | 9.1 |
| Stifle | Tensor fascia latae | **3.1** | *0.5* | **3.1** | *0.5* | **3.1** | *0.5* | 1.3 |
| Stifle | Vastus lateralis | **2.7** | *0.2* | **2.7** | *0.2* | **2.7** | *0.2* | 3.1 |
| Tarsus | Gastrocnemius | **7.7** | *0.2* | **7.7** | *0.2* | **7.7** | *0.1* | 3.1 |
| Tarsus | Peroneus longus | **1.1** | *0.3* | **1.1** | *0.3* | **1.1** | *0.1* | |
| Tarsus | Tibialis caudalis | **0.4** | *0.5* | **0.4** | *0.5* | **0.4** | *0.2* | |
| Tarsus | Tibialis cranialis | **3.6** | *0.2* | **3.6** | *0.2* | **3.6** | *0.1* | 2.2 |

Values are means (bold) and SD (italics).

was measured using electronic scales (EKS, accurate to 0.05 g), and the belly length was measured using a plastic 30 cm ruler or a flexible tape measure (accurate to 1.0 mm). A minimum of three incisions were made into the muscle belly from its origin to its insertion to reveal its constituent fascicles. Ten measurements of fascicle length and three measurements of resting pennation angle (to the nearest degree) were made from random locations throughout the muscle, again using either the 30 cm plastic ruler or flexible tape measure for lengths and a clear plastic protractor for angles.

The muscle volume, physiological cross-sectional area (PCSA), and $F_{max}$ were then calculated. The muscle volume was determined by dividing the mass of the muscle by the muscle density (1.06 g cm$^{-3}$; Mendez & Keys, 1960). The PCSA was calculated as muscle volume/fascicle length, and $F_{max}$ was calculated by multiplying the PCSA by the maximal isometric stress of vertebrate skeletal muscle (0.3 MPa; Wells, 1965; Medler, 2002).

To examine the distribution of muscle mass within the limbs, muscles were grouped according to their function at each joint. Biarticular muscles therefore appear in two categories. Muscle function was determined using the anatomical position and previously published work (Goslow et al. 1973; Williams et al. 2008a,b).

## Muscle moment arms

In cheetah subjects 4–8, muscle moment arms were measured for the major hindlimb muscles, acting at the hip, stifle (equivalent to the human knee) and tarsus (equivalent to the human ankle; see Table 2 for muscles analysed) using the tendon travel method (Landsmeer, 1961; An et al. 1981; Spoor & van Leeuwen, 1992). This method is based on the principle that, if the radius of a circle moves through an angle of $\alpha$ radians, then any point on that radius of a distance, L, from the centre of the circle will have moved through an arc of length

L$\alpha$. In this case, we can consider the joint centre as the centre of the circle, and the arc to be the tendon's path. Therefore, the distance travelled by the tendon (TT) when the joint moves through an angle of one radian is equal to the perpendicular distance between the tendon and the joint centre, or the muscle's moment arm.

$$TT = a\alpha^2 + b\alpha + c$$

The muscle moment arm can therefore be calculated by taking the derivative of TT displacement with respect to joint angle.

$$\frac{dTT}{d\alpha} = 2a\alpha + b$$

Muscle moment arms were measured using the set-up illustrated in Fig. 1. Each muscle was removed, and a length of stiff fishing nylon (30 lb, 0.5 mm diameter, clear nylon Drennan Sea-Thru) was sutured into a stump of muscle or tendon left at its origin or insertion. The nylon was then passed through a small hook that was drilled into the bone at a point estimated as the middle of the origin/insertion of the muscle. A 50 g mass was attached to the free end of the nylon to keep it taut. A marker was then attached to the nylon (between the muscle origin/insertion and hook), and calibration scales glued to each bone. Videos (Sony DCR-SR32E) of the limb were recorded as it moved through three flexion/extension cycles. To facilitate data analysis, contrasting markers were placed on the limb, two on each limb segment to enable calculation of joint angle, two at 4 cm apart for calibration, and one on the hook and one on the marker (located between the hook and muscle origin/insertion) to determine the TT distance.

The videos were processed in custom software written in Matlab (Mathworks v 7.5; Hedrick, 2008) to obtain the x and y
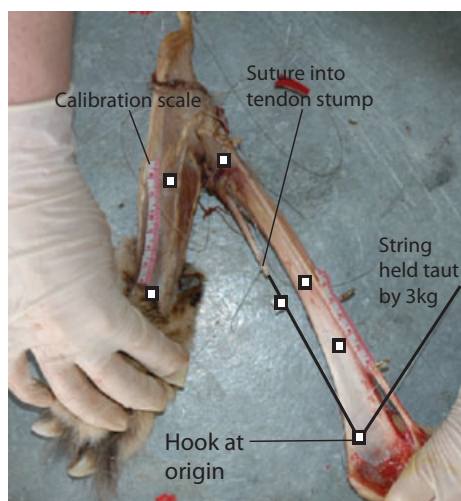
**Fig. 1** Experimental set-up used for collecting moment arms. Two markers were used on each segment to determine the joint angle, two at a 4 cm distance for calibration and two to measure tendon travel.

coordinates for each of the markers. Data were then exported into Excel (Microsoft Office 2007), where the 4 cm calibration distance, TT distances and joint angles were calculated. The joint angle was calculated using the dot product of the vectors between the two markers on each segment. The data were then truncate to represent a realistic range of joint motion during gallop: flexion angles of 45–110° at the hip, 50–115° at the stifle, and 66–178° at the tarsus were determined from kinematics of galloping cheetahs (Hudson PE et al. unpublished data). Midstance moment arms were also examined, with joint angles determined from cheetah galloping kinematics: flexion angles of 80° at the hip, 111° at the stifle and 90° at the tarsus (Hudson et al. unpublished data).

Graphs of joint angle against TT were drawn and either a linear or a second-order polynomial regression was fitted to the data. The best fit was determined using $R^2$ values; however, when both linear and polynomial regressions showed a good fit, with similar $R^2$ values, a linear regression was used. The muscle's moment arm was then obtained by taking the differential of the fitted line. These values were then geometrically scaled to femur length for hip and stifle moment arms and to tibia length for tarsus moment arms to allow comparison between subjects and species.

### Statistical analysis

Species comparisons were made using a Mann–Whitney $U$ test, due to the small number of subjects. Comparisons with $P$ values of < 0.05 were taken to be significant, and instances where $P < 0.01$ are also indicated throughout the Results.

### Results

#### Hindlimb muscle anatomy and architecture

Muscle architecture data were collected from eight cheetahs and three greyhounds. The greyhound data were then combined with six more subjects from previously published work (Williams et al. 2008a,b). No significant differences

existed between the collected greyhound data and the published work. The cheetahs' hindlimb musculature (assuming symmetry between limbs) was found to represent 19.8 ± 2.2% of the total body mass; a similar proportion to the greyhounds at 18.8 ± 2.4% of total body mass.

In total, 37 muscles were measured from the hindlimbs; however, some muscles were missing from the published greyhound data (Table 3). The muscle origins and insertions were identical in the cheetahs and greyhounds, and are shown in Fig. 2. The sole exception was the caudofemoralis muscle, which was only present in the cheetahs, originating from the second and third caudal vertebrae and inserting onto the lateral aspect of the patella via a long tendon. There was a classical proximal to distal distribution of muscle mass throughout the limb with the exception of the small hip rotator muscles (Fig. 3). The heaviest muscle in the cheetahs was the semimembranosus at 332 ± 55 g, whereas in the greyhounds it was the biceps femoris at 460 ± 74 g (Table 3).

Two of the major hip extensors, the biceps femoris and semitendinosus muscles, were approximately one-third lighter in the cheetahs than in the greyhounds ($P < 0.01$). The cheetahs' biceps femoris had a similar fascicle length to that of the greyhounds, and thus a smaller PCSA. The cheetahs' semitendinosus had significantly shorter fascicle length than in the greyhounds and therefore a similar PCSA was observed in both species for this muscle. In contrast, the semimembranosus muscle, another major hip extensor, was significantly ($P < 0.01$) heavier in the cheetahs than the greyhounds and thus, despite little difference in the fascicle length between the species, it had a larger PCSA in the cheetahs. The gluteus medius, a pure hip extensor, exhibited no species differences.

Measurements of the hip flexor muscles, psoas major and psoas minor were obtained for all of the cadavers. The psoas major was extremely well developed in the cheetahs and originates from the ventral aspect of ribs 10–13 and all lumbar vertebrae and inserts onto the lesser trochanter of the femur. It was significantly heavier in the cheetahs than in the greyhounds at 191 ± 46 g and just 52 ± 11 g, respectively, and therefore had a significantly larger PCSA in the cheetahs.

The distribution of distal limb muscle mass is similar between the two species; however, some architectural differences were observed. In particular, the major extensors of the tarsus, the gastrocnemius and superficial digital flexor muscles, both had significantly longer fascicles in the cheetah and therefore a smaller PCSA.

There were several species differences in the masses of functional muscle groups (Fig. 4). Of particular note was the significantly ($P < 0.05$) smaller mass of the hip extensor musculature in the cheetahs when compared with the greyhounds. As many of the hip extensors are biarticular, also functioning to flex the stifle, a similar lower ($P < 0.05$) mass of the stifle flexors was observed. The flexors of the hip

**Table 3** Muscle data: number of subjects (*N*), muscle mass, mean fascicle length and physiological cross-sectional area (PCSA) of the cheetah and greyhound.

| Muscle | N | Cheetah Muscle mass (g) | | Mean fascicle length (cm) | | PCSA (cm$^2$) | | N | Greyhound Muscle mass (g) | | Mean fascicle length (cm) | | PCSA (cm$^2$) | |
|---|---|---|---|---|---|---|---|---|---|---|---|---|---|---|
| Biceps femoris | 8 | 295** | 46.5 | 14.6 | 4.90 | 24.6** | 12.3 | 9 | 460.1 | 74.0 | 14.1 | 3.8 | 39.4 | 23.8 |
| Caudofemoralis | 8 | 69.7** | 9.3 | 14.2 | 3.71 | 5.6 | 1.9 | | | | | | | |
| Sartorius | 8 | 123 | 22.9 | 23.8 | 6.33 | 6.1 | 3.0 | 9 | 155.2 | 110.7 | 21.3 | 6.5 | 8.9 | 6.6 |
| Tensor fascia latae | 8 | 102 | 14.8 | 5.8 | 1.61 | 20.2 | 8.2 | 8 | 82.7 | 33.2 | 6.1 | 4.1 | 19.4 | 8.6 |
| Vastus lateralis | 8 | 214 | 63.2 | 7.6 | 1.85 | 30.7 | 8.7 | 9 | 150.4 | 48.2 | 10.9 | 7.2 | 20.5 | 10.8 |
| Rectus femoris | 8 | 160 | 75.0 | 5.4 | 1.33 | 31.3 | 11.9 | 9 | 204.3 | 144.3 | 7.2 | 4.0 | 32.6 | 20.7 |
| Vastus medialis | 8 | 119 | 19.6 | 6.3 | 1.95 | 22.0 | 5.4 | 9 | 91.9 | 28.6 | 4.4 | 1.5 | 24.9 | 11.2 |
| Vastus intermedius | 8 | 38.1** | 24.4 | 6.5 | 2.01 | 7.1 | 5.3 | 9 | 69.5 | 26.1 | 7.0 | 5.3 | 16.3 | 14.2 |
| Semitendinosus | 8 | 121** | 29.5 | 10.0** | 1.38 | 13.1 | 4.5 | 9 | 176.2 | 80.4 | 16.1 | 4.5 | 12.6 | 6.1 |
| Semimembranosus | 7 | 332** | 55.4 | 25.4 | 6.39 | 15.0 | 5.8 | 9 | 200.1 | 76.1 | 22.0 | 3.6 | 9.7 | 3.8 |
| Gracilis | 8 | 114 | 28.7 | 7.1 | 3.01 | 20.4 | 10.2 | 9 | 144.4 | 74.0 | 6.5 | 4.6 | 32.9 | 27.1 |
| Gluteal superficialis | 8 | 28.4** | 4.5 | 7.2 | 3.81 | 5.3 | 3.4 | 8 | 115.7 | 79.1 | 5.8 | 1.5 | 25.7 | 21.5 |
| Gluteus medius | 8 | 136 | 18.0 | 6.4 | 1.18 | 23.4 | 7.1 | 9 | 134.7 | 73.2 | 5.7 | 2.1 | 27.9 | 17.6 |
| Gluteus profundus | 8 | 17.6* | 4.5 | 2.9 | 0.61 | 6.7 | 2.4 | 6 | 31.4 | 16.2 | 4.3 | 1.6 | 7.7 | 2.3 |
| Piriformis | 8 | 17.3 | 4.4 | 2.9 | 0.88 | 7.4 | 4.7 | 3 | 12.6 | 0.7 | 2.4 | 0.6 | 5.8 | 1.8 |
| Gemelli | 8 | 19.4 | 16.3 | 2.0* | 0.81 | 10.4 | 8.7 | 3 | 11.3 | 3.8 | 4.7 | 2.1 | 3.1 | 1.9 |
| Quadratus femoris | 8 | 13.6 | 1.1 | 4.3* | 1.02 | 3.5 | 1.0 | 3 | 13.8 | 1.1 | 5.8 | 1.2 | 2.6 | 0.5 |
| Obturator externus | 7 | 28.7 | 13.1 | 2.8 | 0.90 | 11.4 | 5.3 | 3 | 15.9 | 1.0 | 2.5 | 0.8 | 7.2 | 2.8 |
| Obturator internus | 8 | 36.5 | 11.3 | 2.9 | 0.50 | 13.7* | 4.7 | 3 | 16.2 | 2.6 | 2.3 | 0.3 | 7.4 | 0.4 |
| Pectinius | 7 | 30.9 | 23.8 | 5.3 | 3.33 | 5.6** | 1.5 | 9 | 24.7 | 16.9 | 2.0 | 0.8 | 15.6 | 12.1 |
| Adductor magnus | 7 | 316 | 63.2 | 16.0 | 4.30 | 22.9 | 8.9 | 3 | 238.6 | 70.2 | 16.5 | 3.6 | 15.3 | 3.9 |
| Adductor brevis | 7 | 103 | 11.9 | 11.6 | 3.40 | 10.3 | 3.8 | 3 | 92.3 | 11.1 | 12.3 | 1.8 | 8.1 | 2.0 |
| Illiacus | 7 | 14.4 | 4.0 | 5.7 | 3.22 | 3.1 | 1.9 | 3 | 13.9 | 8.7 | 4.4 | 1.3 | 3.1 | 1.6 |
| Psoas major | 8 | 191* | 45.9 | 13.9 | 4.39 | 16.4* | 7.5 | 3 | 52.0 | 11.2 | 9.7 | 0.2 | 5.7 | 1.3 |
| Psoas minor | 8 | 44.1 | 4.6 | 4.8 | 1.18 | 10.4 | 3.2 | 3 | 32.5 | 15.0 | 6.5 | 2.9 | 6.6 | 4.9 |
| Gastrocnemius – lateral | 8 | 31.1 | 6.7 | 2.5* | 0.82 | 13.9** | 3.9 | 9 | 33.9 | 15.8 | 1.6 | 0.5 | 22.4 | 8.3 |
| Gastrocnemius – medial | 8 | 47.1 | 8.7 | 2.8* | 0.61 | 18.3** | 5.2 | 9 | 43.4 | 10.6 | 1.7 | 0.7 | 30.6 | 11.9 |
| Superficial digital flexor | 8 | 65.1 | 10.0 | 2.4 | 0.74 | 30.7 | 10.9 | 9 | 55.5 | 18.7 | 1.9 | 1.0 | 41.4 | 35.0 |
| Soleus | 5 | 16.0 | 7.0 | 2.4 | 0.84 | 8.2 | 4.9 | 3 | 9.5 | 2.3 | 1.8 | 0.6 | 5.9 | 1.1 |
| Long digital extensor | 8 | 40.5* | 6.7 | 7.5 | 2.26 | 6.2 | 2.1 | 9 | 31.3 | 8.9 | 5.9 | 4.0 | 9.4 | 8.7 |
| Tibialis cranialis | 8 | 39.3 | 7.1 | 8.8 | 2.75 | 5.3 | 2.3 | 3 | 29.3 | 4.6 | 10.4 | 1.4 | 3.1 | 0.8 |
| Popliteus | 8 | 14.8 | 4.3 | 2.3 | 0.57 | 7.1 | 2.9 | 9 | 13.8 | 6.7 | 3.2 | 1.4 | 5.6 | 3.9 |
| Lateral digital extensor | 7 | 4.71 | 1.1 | 2.6 | 1.00 | 2.3 | 1.4 | 3 | 4.1 | 3.4 | 2.4 | 0.6 | 1.6 | 1.0 |
| Peroneous longus | 7 | 10.4 | 4.1 | 3.2 | 0.90 | 3.9* | 2.0 | 9 | 16.5 | 10.6 | 2.2 | 1.0 | 9.0 | 6.4 |
| Peroneous brevis | 3 | 2.20 | 2.4 | 1.3 | 1.26 | 1.6 | 0.3 | 3 | 1.0 | 0.0 | 0.4 | 0.1 | 3.2 | 1.0 |
| Deep digital flexor – medial | 7 | 31.0* | 4.5 | 2.9 | 0.61 | 12.2 | 3.3 | 3 | 12.9 | 1.9 | 3.1 | 1.7 | 5.4 | 3.2 |
| Deep digital flexor – lateral | 7 | 32.3 | 7.9 | 3.4 | 0.60 | 10.2 | 2.9 | 3 | 18.0 | 3.0 | 2.4 | 0.8 | 8.9 | 3.9 |
| Caudal tibial | 6 | 10.0 | 4.0 | 3.5 | 0.84 | 3.1 | 1.4 | 3 | 5.7 | 2.1 | 2.8 | 0.6 | 2.3 | 1.1 |

BF, biceps femoris; CF, caudofemoralis; Sar, sartorius; TFL, tensor fascia latae; VL, vastus lateralis; RF, rectus femoris; VM, vastus medialis; VI, vastus intermedius; SemiT, semitendinosus; SemiM, semimembranosus; Grac, Gracilis; GS, gluteal superficialis; GM, gluteus medius; GP, gluteus profundus; Piri, piriformis; Gem, gemelli; QF, quadratus femoris; ObEx, obturator externus; ObInt, obturator internus; Pect, pectinius; AdMag, adductor magnus; AdBrev, adductor brevis; Il, illiacus; Pmaj, psoas major; Pmin, psoas minor; Glat, gastrocnemius – lateral; Gmed, gastrocnemius – medial; SDF, superficial digital flexor; Sol, soleus; LongDE, long digital extensor; Tcra, tibialis cranialis; Pop, popliteus; Edlat, lateral digital extensor; PL, peroneous longus; PB, peroneous brevis; DDFmed, deep digital flexor – lateral; DDFlat, deep digital flexor – lateral; Tcau, caudal tibial; Gast, gastrocnemius; Vlat, vastus lateralis; Plong, peroneus longus.

Values indicate mean (bold) and SD (italics). A Mann–Whitney *U* test was performed to test for significant species differences with *P < 0.05 and **P < 0.01.
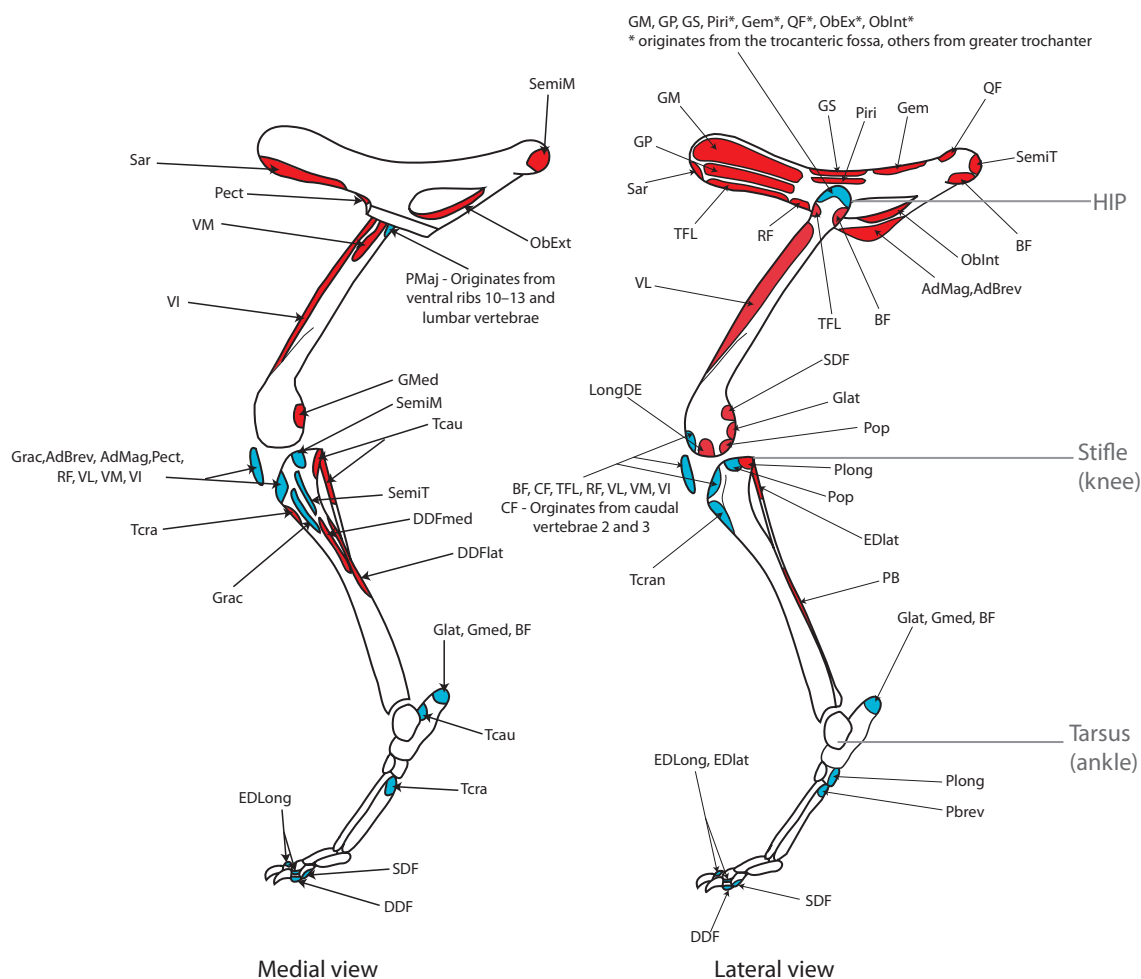
**Fig. 2** Schematic illustration of muscle origins and insertions in the cheetah. Origins are in red and insertions in blue. Muscle name abbreviations are given in Table 3.

were significantly ($P < 0.01$) heavier in the cheetahs than the greyhounds.

## Hindlimb muscle moment arms

Muscle moment arms were measured for five cheetahs (subjects 4–8) and compared with four greyhounds from previously published work (Williams et al. 2008a,b). Unfortunately, results for individual greyhound subjects were unavailable and so the published means will be used for comparison. The moment arms of six muscles that function at the hip, seven at the stifle and four at the tarsus were measured. Maximum and minimum moment arm values are given in Table 2, along with the moment arm at mid-stance. Figure 5 shows a comparison between the moment arms of the cheetahs and greyhounds when geometrically scaled.

Many of the hindlimb muscles showed a variation in moment arm length with changes in joint angle; the largest variation was observed in those functioning at the hip. All

of the hip extensors, biceps femoris, semimembranosus and semitendinosus, had longer moment arms in the cheetahs than in the greyhounds. At the stifle and tarsus, the cheetahs' muscles had proportionally longer moment arms than the greyhounds.

## Hindlimb skeleton and pelvis

The hindlimb skeleton of the cheetahs showed several unique features. Of particular note was the cheetahs' pelvis, which was long and narrow, largely due to an elongated ischium when compared with that of the greyhounds (Fig. 6A,B). The cheetahs also had more divergent talar ridges at the tarsus (these articulate with the tibia) (Fig. 6C,D) and an elongated calcaneus (Fig. 6C,D). The cheetahs' femur had a mean length of $87 \pm 4$ mm kg$^{1/3}$ (mean ± SE), which was proportionally longer ($P < 0.05$) than that of the greyhounds at $69 \pm 3$ mm kg$^{1/3}$ (Table 1). Unfortunately, no published values exist for limb bone mass and mid-shaft diameter in greyhounds, and therefore only
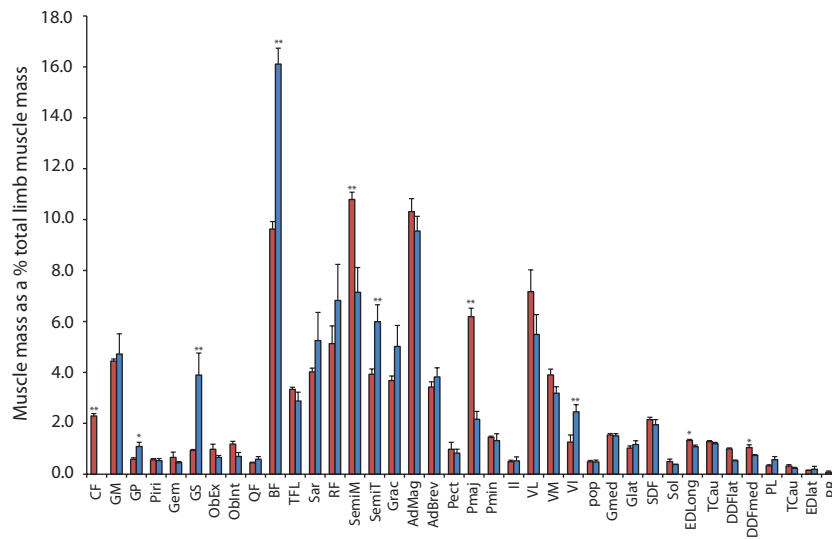
**Fig. 3** Proximal to distal distribution of muscle mass. Bars are representative of means + SE. Species comparison made by performing a Mann–Whitney $U$ test (*$P < 0.05$; **$P < 0.01$). Cheetah values are in red and greyhound values in blue. Muscle name abbreviations are given in Table 3.
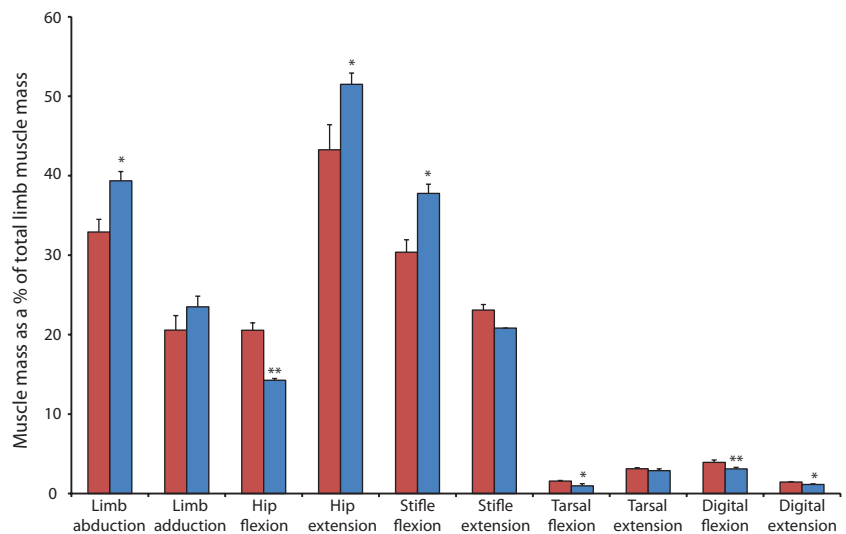


**Fig. 4** Functional distribution of muscle mass. Bars are means + SEs. Species comparison made by performing a Mann–Whitney $U$ test (*$P < 0.05$; **$P < 0.01$). Cheetah values are in red and greyhound values in blue.

data for the three greyhounds dissected in this study were available. Because of this, no statistical comparison was possible; however, when scaled geometrically, the cheetahs appear to have a heavier femur and tibia than the greyhounds, but only the cheetahs' femur had a larger midshaft diameter.

## Discussion

The muscle architecture, moment arms and skeleton of the pelvic limb of the cheetah and greyhound were quantified and compared. This enabled us to investigate differences and adaptations that may account for the cheetah's higher top speed, despite their similarities in mass and gross morphology. The hindlimb musculature of both animals comprised a large proportion of their total body mass. In the

cheetah this is particularly large at 19.8 ± 2.2% compared with other high-speed quadrupedal mammals [hare, 16.3 ± 0.9% (Williams et al. 2008a,b) and horse, 18.8 ± 2.9% (Payne et al. 2005) of body mass]. The cheetah and greyhound have identical gross muscular anatomy with the exception of the caudofemoralis muscle, which functions to flex the tail laterally, extend the hip and abduct the limb. This muscle is present in all felids and not in canids.

### Limb length

The femur ($P < 0.05$) and tibia were both proportionally longer in the cheetah than in the greyhound, suggesting that the cheetah had a proportionally longer hindlimb. A recent study (Day & Jayne, 2007) has shown the cheetah to have a proportionally longer hindlimb than a variety of
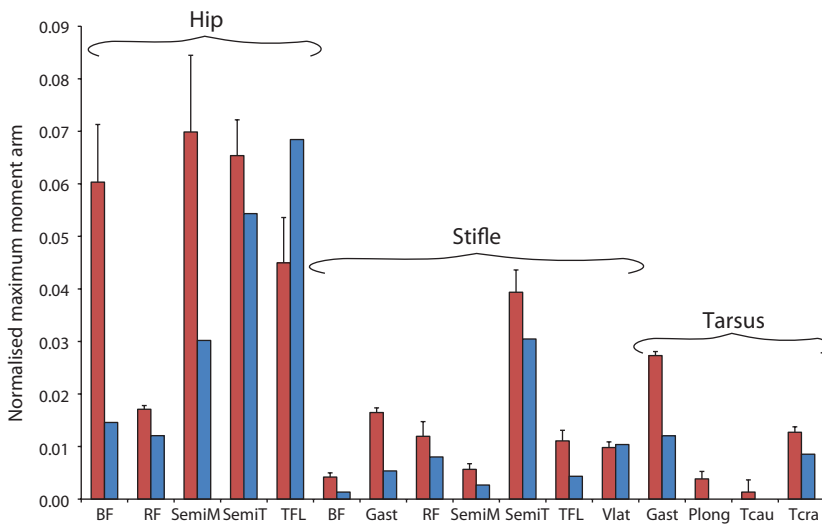
**Fig. 5** Maximum moment arms of muscles functioning at the hip, stifle and tarsus in the cheetah (red) and greyhound (blue) (Williams et al. 2008a,b). Bars represent means + SEs. Only means were available for the greyhound.
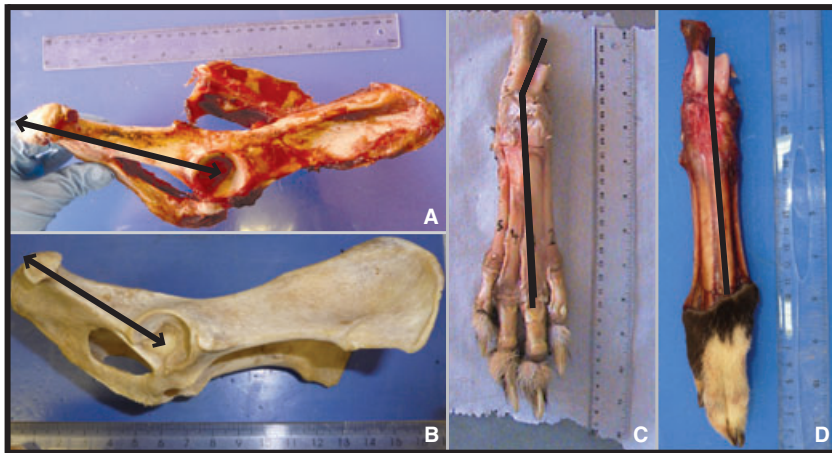


**Fig. 6** Skeletal morphology. (A) Cheetah and (B) greyhound: the lateral aspect of the pelvis, with the black arrows illustrating the elongated ischium in the cheetah. (C) Cheetah and (D) greyhound: the dorsal aspect of the hindfeet with the black line illustrating the increased angle of divergence of the talar ridges (which articulate with the tibia) in the cheetah.

other felids; however, the values for limb bone lengths in that study were significantly greater than those measured here. This may be due to differences in method. In the study of Day & Jayne (2007), limb bone lengths were measured from video rather than by direct measurement through cadaveric dissection, highlighting the differences between limb segment lengths and bone lengths.

A longer hindlimb should enable the cheetah to increase its stride length and therefore its speed (assuming that it causes no increase in swing times). It will also enable a longer contact length (the distance that the centre of mass moves whilst the foot is in contact with the ground), allowing the cheetah to use longer contact times than the greyhound. This will allow the cheetah to maintain higher duty factors (the proportion of the stride in which the feet are in contact with the ground), and therefore use lower peak limb forces than the greyhound, at a given speed. This may contribute to the cheetah achieving higher top speeds. Despite these apparent advantages, there are several disadvantages to having a longer limb. For example, the chee-

tahs' femur and tibia were also heavier and had a larger mid-shaft diameter, characteristics necessary to maintain the bones' strength and safety factors with increasing length (Alexander, 1993; Sorkin, 2008). This would theoretically increase the inertia of the limb, and it would therefore require more muscular work to accelerate, decelerate and swing the cheetah limb. However, a study comparing the energetic cost of running in three different species of quadruped identified very little difference in the energetic cost of running due to variations in limb configuration (Taylor et al. 1974). Despite this, the energetic cost of swinging its limb will not be of primary importance to the cheetah. For its high speed sprint the ability to rapidly swing and reposition its limbs will be more crucial.

### Skeletal specialisations

The cheetahs exhibited three major differences in skeletal morphology when compared with the greyhounds. Firstly, there was the elongation of the ischium of the pelvis, which

provided the hip extensor muscles with a longer moment arm about the hip, thereby increasing the joint torques that these muscles can achieve. Secondly, there were the divergent talar ridges, which resulted in a degree of external rotation of the pes on flexion of the tarsus, moving the pes laterally away from the body. This could potentially help to avoid interference between the hindlimbs and forelimbs in the gathered aerial phase of the cheetah's gait when the forelimbs and hindlimbs cross over. Finally, there was an elongation of the calcaneus, which would provide the extensor muscles of the tarsus with a longer moment arm, thereby increasing the joint torque that they can achieve.

## Comparative hindlimb anatomy and function

A classical proximal to distal reduction in muscle mass was observed in both species, with the bulk of the hindlimb musculature located close to the hip joint (Payne et al. 2005). This will significantly reduce the swing inertia of the hindlimbs, reducing the amount of muscular work required to accelerate and decelerate the limb (Lee et al. 2004). This may aid in achieving faster swing times and therefore higher stride frequencies and increased speed. To examine the distribution of muscle mass within their limbs more closely, muscles were grouped according to their function (Fig. 4).

Although the functional distribution of muscle mass was similar between the two species, some surprising differences did exist. It was hypothesised that cheetahs would have a larger volume of hip extensor musculature to provide the power needed to accelerate their centre of mass rapidly (Williams et al. 2008a,b), yet the present study showed that cheetahs have proportionally less hip extensor musculature than greyhounds ($P < 0.05$). This is mainly due to the lighter biceps femoris and semitendinosus muscles; however, one of the pure hip extensor muscles, gluteus medius, exhibited no species differences in either mass or architecture. When comparing the gluteus medius of greyhounds and mixed-breed dogs, again no species variation was found (Williams, 2008), and thus its size may be constrained by its position within the limb. The hip extensor muscles of the cheetah have an architecture and moment arms suitable for producing large joint torques (Fig. 7B); however, due to their smaller mass and therefore volume, they would be less powerful (Fig. 7A). Powerful hip extensors are crucial for accelerating rapidly (Williams et al. 2009a,b), a skill at which both cheetahs (Marker & Dickman, 2003) and racing greyhounds (Williams et al. 2009a,b) are adept. We theorise that cheetahs power acceleration using their extensive back musculature, potentially through both passive and active mechanisms (Alexander et al. 1985; Alexander, 1988; Ritter et al. 2001). If this is the case, then large hip extensor torques will be required to resist motion⁄extend the hip to enable forward propulsion of the centre of mass. Despite the significance of this result, it may simply be an effect of our cheetah subjects being captive animals and our greyhounds being physically active and racing until death (see study limitations below).

The flexors of the hip were significantly heavier in the cheetahs than in the greyhounds ($P < 0.01$), due to the psoas major muscle being over three times heavier in the cheetahs. This muscle's large volume, PCSA and long fascicle lengths make it suitable for high power outputs. This will enable cheetahs to rapidly protract their hindlimbs. We also suggest that the psoas muscle possibly acts to resist pitching moments about the hips that occur during rapid accelerations (Williams et al. 2009a,b), helping to maintain the body in a horizontal position.

In the distal limb, the majority of muscles were of a similar mass in both species but, when grouped by function, cheetahs had significantly larger muscle mass for tarsal flexion, digital flexion and digital extension. The gastrocnemius muscles had a similar mass in both species, but the cheetahs had longer fascicles and therefore a smaller PCSA. Despite this, the elongated calcaneus in the cheetahs provides the gastrocnemius with a longer moment arm at the tarsus enabling it to generate much larger joint torques than in the greyhounds (Fig. 7B). The gastrocnemius is a biarticular muscle also functioning to flex the stifle (where we also see an elongated moment arm in the cheetah; Fig. 7B). This muscle is active during the stance phase when the tarsus and stifle flex (Goslow et al. 1973, 1981) and acts to resist the large ground reaction force joint moment that exists at the tarsus (Colborne et al. 2006).

## Study limitations

This study represents the most complete investigation into the anatomy of the cheetah; however, several limitations must be acknowledged. The cheetahs were captive, albeit in large enclosures enabling them the opportunity to run but unlikely at high speeds, and had died of natural causes and therefore some alterations in architecture associated with lack of exercise must be assumed (Blazevich et al. 2003). Lack of exercise would not affect the origins and insertions of the muscles, nor their moment arms, and thus the significance of these results is unaffected.

The quantification of muscle anatomy will inherently have errors; however, we believe our results to be a good indication of muscle function. Such errors include muscle fibre shrinkage that can occur due to rigor mortis and the freezing process (Cutts, 1988), as well as the calculation of PCSA. The calculated PCSA of a muscle will be affected by the pennation angle ($\theta$) of its fibres, such that PCSA = (muscle mass × cos $\theta$)⁄(muscle density × fibre length). In this study, the majority of pennation angles were around 30° or less, and therefore cos $\theta$ will be close to 1. Such pennation angles will therefore have a small effect on the calculated PCSA of the muscles (Calow & Alexander, 1973). Pennation angles also vary significantly during contraction (Muhl,
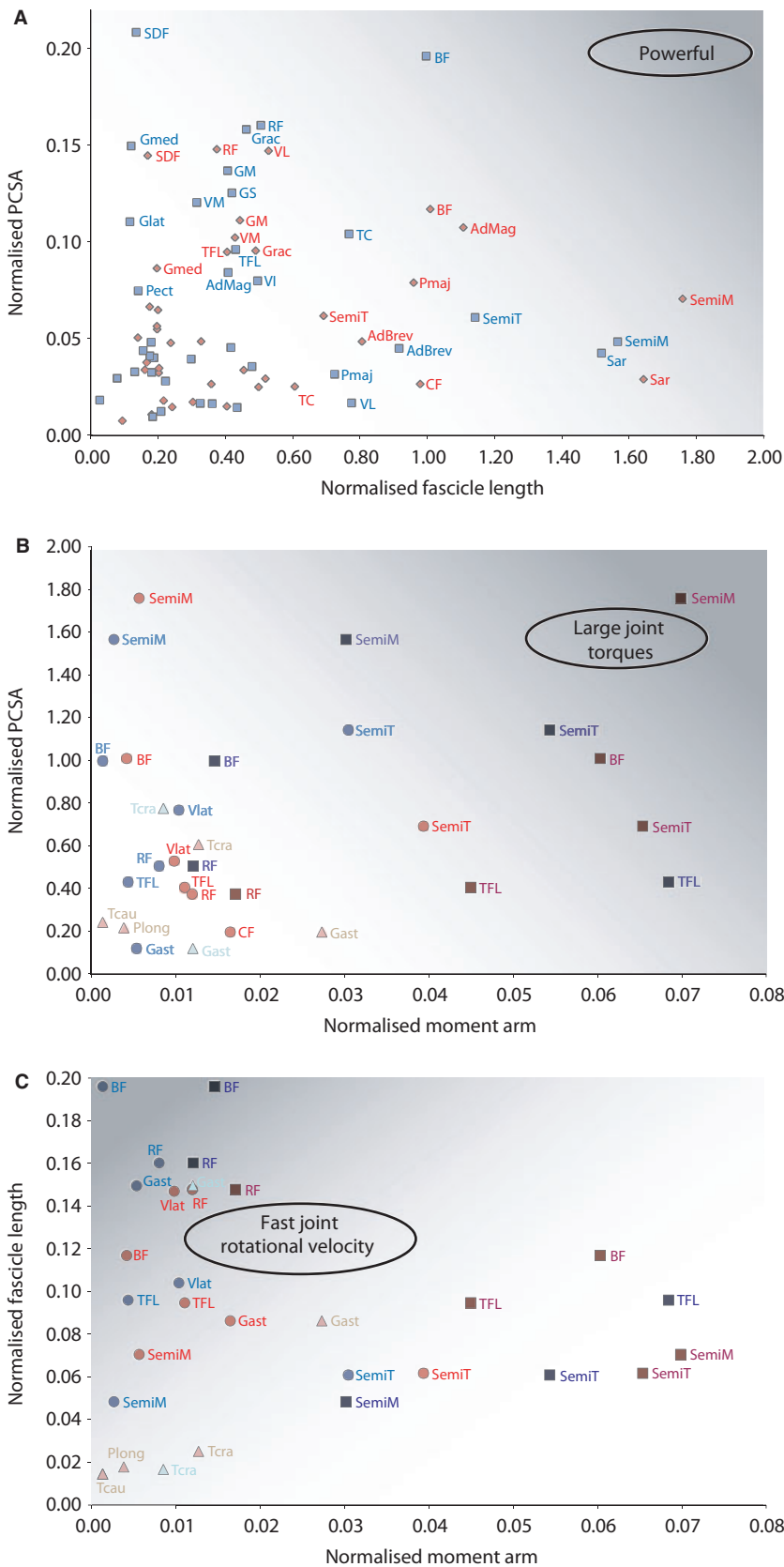
Fig. 7 (A) Physiological cross-sectional area (PCSA) against fascicle length to illustrate the balance between force, range of motion/velocity and power output for different muscles. All architectural data was normalised geometrically to total limb muscle mass. (B) Moment arm against PCSA to illustrate the muscle's ability to produce large joint moments. (C) Moment arm against fascicle length to illustrate the muscle's ability to rotate the joint rapidly. All moment arm data were normalised to bone lengths. Darker shaded areas of the graphs represent increased power output (A), large joint torques (B) and faster joint rotational velocity (C). Cheetah values are represented in red and greyhound values in blue. In (B) and (C), muscles acting at the hip are represented by squares, those acting at the stifle by circles, and those acting at the tarsus by triangles. Muscle name abbreviations are given in Table 3.

1982; Lichtwark et al. 2007; Azizi et al. 2008) and so the measured pennation angles may not be representative of the angles in life. We therefore decided to ignore the effect of pennation angle on the calculation of PCSA, and simply use our measurements of pennation angle for qualitative description of muscle architecture and function.

Several methods exist to measure muscle moment arms, such as imaging (Hughes et al. 1997; Juul-Kristensen et al. 2000; Graichen et al. 2001) or simply estimating the distance from the joint centre to the muscle's line of action (Nemeth & Ohlsen, 1985), both of which require knowledge of the exact position of the joint centre. This is particularly difficult to determine and may vary depending on joint angle (Smith et al. 2007). In the present study we used the tendon travel method for measurement of moment arms, avoiding the need to accurately determine the joint centre; however, inaccuracies remain and large variation can occur with biarticular muscles depending on the posture of one of the joints whilst measurements are taken at the other (MacFadden & Brown, 2007). When measuring biarticular muscle moment arms in our experiments, we aimed to hold the joint not being measured in an extended posture; however, in future it could prove more accurate to move the entire limb through the angles that they experience during stance simultaneously.

## Conclusions

In conclusion, we have quantified the hindlimb anatomy of the cheetah and compared it with both our own and previously published data on the racing greyhound, identifying features that may explain how cheetahs attain a higher maximum speed.

**1** The cheetah exhibits several unique skeletal adaptations that mostly act to increase muscle moment arms when compared with the greyhound. The cheetah also possesses divergent talar ridges, an adaptation that may help to prevent limb interference during the gathered aerial phase of the gallop.

**2** The cheetah has significantly longer hindlimb bones than the greyhound, enabling it to have a longer contact length and potentially an increased stride length. The cheetah's limb bones are also proportionally heavier and have a larger mid-shaft diameter, suggesting that they are suited for resisting larger forces.

**3** The cheetah has a smaller volume of muscle at the hip than the greyhound, and thus is unable to obtain the power required for acceleration from hip extensor musculature alone. We hypothesise that the additional power is generated by the substantial amount of back musculature that the cheetah possesses.

**4** The cheetah has particularly large psoas muscles, which we suggest are used to rapidly protract the hindlimb, and to resist pitching moments about the hip that occur during accelerations.

## Author contributions

The experiments were designed and planned by all authors. P.E.H., S.N.C., S.A.C., E.L. and R.C.P.-D. helped with data collection and analysis. P.E.H. wrote the paper with input from S.A.C. and A.M.W.

## References

Alexander RM (1988) Why Mammals Gallop 1. *Integr Comp Biol* **28**, 237–245.

Alexander RM (1993) Optimization of structure and movement of the legs of animals. *J Biomech* **26**(Suppl. 1), 1–6.

Alexander RM (2003) *Principles of Animal Locomotion*. Princeton: Princeton University Press.

Alexander RMN, Jayes AS (1978) Vertical movements in walking and running. *J Zool Lond* **185**, 27–40.

Alexander RM, Dimery NJ, Ker RF (1985) Elastic structures in the back and their role in galloping in some mammals. *J Zool* **207**, 467–482.

An KN, Hui FC, Morrey BF, et al. (1981) Muscles across the elbow joint: a biomechanical analysis. *J Biomech* **14**, 659–661.

Azizi E, Brainerd EL, Roberts TJ (2008) Variable gearing in pennate muscles. *PNAS* **105**, 1745.

Blazevich AJ, Gill ND, Bronks R, et al. (2003) Training-specific muscle architecture adaptation after 5-wk training in athletes. *Med Sci Sports Exerc* **35**, 2013–2022.

Calow LJ, Alexander RM (1973) A mechanical analysis of a hind leg of a frog (*Rana temporaria*). *J Zool Lond* **171**, 293–321.

Colborne GR, Walker AM, Tattersall AJ, et al. (2006) Effect of trotting velocity on work patterns of the hind limbs of Greyhounds. *Am J Vet Res* **67**, 1293–1298.

Cutts A (1988) Shrinkage of muscle fibres during the fixation of cadaveric tissue. *J Anat* **160**, 75–78.

Day LM, Jayne BC (2007) Interspecific scaling of the morphology and posture of the limbs during the locomotion of cats (Felidae). *J Exp Biol* **210**, 642–654.

Goslow GE, Reinking RM, Stuart DG (1973) The cat step cycle: hind limb joint angles and muscle lengths during unrestrained locomotion. *J Morphol* **141**, 1–41.

Goslow GE, Seeherman HJ, Taylor CR, et al. (1981) Electrical activity and relative length changes of dog limb muscles as a function of speed and gait. *J Exp Biol* **94**, 15–42.

Graichen H, Englmeier KH, Reiser M, et al. (2001) An in vivo technique for determining 3D muscular moment arms in

different joint positions and during muscular activation – application to the supraspinatus. *Clin Biomech* **16**, 389–394.

Hedrick TL (2008) Software techniques for two- and three-dimensional kinematic measurements of biological and biomimetic systems. *Bioinspir Biomim* **3**, 034001.

Hughes RE, Niebur G, Liu J, et al. (1997) Comparison of two methods for computing abduction moment arms of the rotator cuff. *J Biomech* **31**, 157–160.

Juul-Kristensen B, Bojsen-Møller F, Holst E, et al. (2000) Comparison of muscle sizes and moment arms of two rotator cuff muscles measured by ultrasonography and magnetic resonance imaging. *Eur J Ultrasound* **11**, 161–173.

Landsmeer JM (1961) Studies in the anatomy of articulation. II. Patterns of movement of bi-muscular, bi-articular systems. *Acta Morphol Neerl Scand* **3**, 304–321.

Lee DV, Stakebake EF, Walter RM, et al. (2004) Effects of mass distribution on the mechanics of level trotting in dogs. *J Exp Biol* **207**, 1715–1728.

Litchwark GA, Bougoulias K, WIlson AM (2007) Muscle fascicle and series elastic element length changes along the length of the human gastrocnemius during walking and running. *J Biomech* **40**, 157–164.

MacFadden LN, Brown NA (2007) Biarticular hip extensor and knee flexor muscle moment arms of the feline hindlimb. *J Biomech* **40**, 3448–3457.

Marker LL, Dickman AJ (2003) Morphology, physical condition, and growth of the cheetah (*Acinonyx jubatus*). *J Mammol* **84**, 840–850.

Medler S (2002) Comparative trends in shortening velocity and force production in skeletal muscles. *Am J Physiol Regul Integr Comp Physiol* **283**, R368–R378.

Mendez J, Keys A (1960) Density and composition of mammalian muscle. *Metabolism* **9**, 184–188.

Muhl ZF (1982) Active length-tension relation and the effect of muscle pinnation on fiber lengthening. *J Morphol* **173**, 285–292.

Nemeth G, Ohlsen H (1985) In vivo moment arm lengths for hip extensor muscles at different angles of hip flexion. *J Biomech* **18**, 129.

Payne RC, Hutchinson JR, Robilliard JJ, et al. (2005) Functional specialisation of pelvic limb anatomy in horses (Equus caballus). *J Anat* **206**, 557–574.

Ritter DA, Nassar PN, Fife M, et al. (2001) Epaxial muscle function in trotting dogs. *J Exp Biol* **204**, 3053–3064.

Sharp N (1997) Timed running speed of a cheetah (*Acinonyx jubatus*). *J Zool Lond* **241**, 493–494.

Smith NC, Wilson AM, Jespers KJ, et al. (2006) Muscle architecture and functional anatomy of the pelvic limb of the ostrich (Struthio camelus). *J Anat* **209**, 765–779.

Smith NC, Payne RC, Jespers KJ, et al. (2007) Muscle moment arms of pelvic limb muscles of the ostrich (Struthio camelus). *J Anat* **211**, 313–324.

Sorkin B (2008) Limb bone stresses during fast locomotion in the African lion and its bovid prey. *J Zool Lond* **276**, 213–218.

Spoor CW, van Leeuwen JL (1992) Knee muscle moment arms from MRI and from tendon travel. *J Biomech* **25**, 201–206.

Taylor CR, Shkolnik A, Dmi'el R, et al. (1974) Running in cheetahs, gazelles, and goats: energy cost and limb configuration. *Am J Physiol* **227**, 848–850.

Usherwood JR, Wilson AM (2005) Biomechanics: no force limit on greyhound sprint speed. *Nature* **438**, 753–754.

Wells JB (1965) Comparison of mechanical properties between slow and fast mammalian muscles. *J Physiol* **178**, 252–269.

Williams SB, Wilson AM, Daynes J, et al. (2008a) Functional anatomy and muscle moment arms of the thoracic limb of an elite sprinting athlete: the racing greyhound (*Canis familiaris*). *J Anat* **213**, 373–382.

Williams SB, Wilson AM, Rhodes L, et al. (2008b) Functional anatomy and muscle moment arms of the pelvic limb of an elite sprinting athlete: the racing greyhound (*Canis familiaris*). *J Anat* **213**, 361–372.

Williams SB, Tan H, Usherwood JR, et al. (2009a) Pitch then power: limitations to acceleration in quadrupeds. *Biol Lett* **5**, 610–613.

Williams SB, Usherwood JR, Jespers K, et al. (2009b) Exploring the mechanical basis for acceleration: pelvic limb locomotor function during accelerations in racing greyhounds (*Canis familiaris*). *J Exp Biol* **212**, 550–565.

Witte TH, Hirst CV, Wilson AM (2006) Effect of speed on stride parameters in racehorses at gallop in field conditions. *J Exp Biol* **209**, 4389–4397.

Zajac FE (1989) Muscle and tendon: properties, models, scaling, and application to biomechanics and motor control. *Crit Rev Biomed Eng* **17**, 359–411.